

RESEARCH PAPER

Synthesis, Characterization and Antibacterial Activity of Copper(II) Metal-Organic Nanocapsule

Mojdeh Nakhaei, Kamran Akhbari*

School of Chemistry, College of Science, University of Tehran, Tehran, Iran.

ARTICLE INFO

Article History:

Received 04 July 2020

Accepted 20 September 2020

Published 15 October 2020

Keywords:

Biomedical applications

Nanoparticles

Copper

Nanocapsule

Sonochemical

ABSTRACT

The antibacterial activity of a metal-organic nanocapsule $[\text{Cu}_2(\text{dpa})_2(\text{bpy})_2]\cdot 4\text{H}_2\text{O}$ (**1**), (H_2dpa = diphenyl-2,2'dicarboxylic acid and bpy = 2,2' bipyridine) was investigated against gram-positive and gram-negative bacterial strains. First, $[\text{Cu}_2(\text{dpa})_2(\text{bpy})_2]\cdot 4\text{H}_2\text{O}$ was synthesized by both the reflux and sonochemical processes. Then, the obtained products were characterized by powder X-ray diffraction (PXRD), IR spectroscopy and scanning electron microscopy (SEM). Finally, their antibacterial performance was investigated by the agar well diffusion method. The results showed that the compound is active against *S. aureus*, whereas, it is inert against *E. coli* bacteria. The fact that bpy exhibited a high antibacterial performance against *E. coli*, while compound **1** samples were inert against *E. coli* bacteria shows that ligand release in metal-organic nanocapsule of **1** does not occur. It seems that the mechanism of compound **1** for its antibacterial activity is different from other reported compounds and is not attributed to Cu^{2+} and ligand release from **1**, because of its high chemical stability.

How to cite this article

Nakhaei M., Akhbari K. Synthesis, Characterization and Antibacterial Activity of Copper(II) Metal-Organic Nanocapsule. Nanochem Res, 2020; 5(2):225-232. DOI: 10.22036/nrcr.2020.02.012

INTRODUCTION

Contamination by pathogens is an important issue in different areas such as food industry, medical devices, healthcare, hygienic applications, treatment of infectious disease, textiles, water purification systems, etc [1-5]. Also, the rising resistance of microorganisms towards antibiotic drugs has become an issue in recent years. Thus, various research efforts have been made to discover novel antimicrobial agents [6]. The antibacterial performance of transition metals such as copper (Cu), silver (Ag), zinc (Zn), gold (Au) and titanium (Ti) and also their nano-particles (NPs) has been discovered and applied as substitutes for some traditional disinfectants. Metallic NPs have exhibited a great antibacterial activity due to increase in their surface area with the decrease in the particle size. However, metallic NPs are

toxic to normal tissues as well as to pathogen microorganisms. So, it is necessary to investigate safer biocidal materials [7-12]. Cu nanoparticles have particular biological, chemical and physical features. It is an essential trace element in animal and plant tissues and has some vital roles in the human body, such as synthesis of some proteins, activating energy production in cells, and the formation of nervous tissue. Also, it has gained attention as an antibacterial agent because it is cheaper compared with other antibacterial metallic NPs. In previous studies, Cu has exhibited high potential antimicrobial effects [13-15]. The mechanism introduced for Cu nanoparticles is that Cu ions cross from the bacterial cell membrane and damage the vital enzymes [6, 14]. Another highly popular materials discovered as antibacterial agents are hybrid organic-inorganic compounds. Antibacterial activity of these compounds is

* Corresponding Author Email: akhbari.k@khayam.ut.ac.ir

originated from the release of metal ions. The studies have shown that the cytotoxicity of the antibacterial agents decreases when the biocides are released slowly. The benefit of using hybrid organic-inorganic compounds as the antimicrobial agents is that the release of the antimicrobial agent is more controllable [13, 16]. Metal-organic nanocapsules (MONCs) are a branch of hybrid organic-inorganic compounds. Capsules are determined as reservoirs that their hollow or soft material-filled cavities are surrounded by a shell of solid materials. Metal-organic nanocapsules have interesting properties such as low density, due to their structures. Supramolecular nanocapsules have gained attraction owing to their cavities for encapsulating the guest molecules. The structural cavity of MONCs provides potential applications in a variety of areas such as enclosing dye or pigment, heterogeneous catalysis, drug or gene delivery, removal of hazardous material, etc [17-24]. Based on our literature review, MONCs have not been investigated as antibacterial agents. Herein, the antimicrobial effect of the bulk and nanosized samples of the $[\text{Cu}_2(\text{dpa})_2(\text{bpy})_2]\cdot 4\text{H}_2\text{O}$ (**1**) metal-organic nanocapsule [25], (H_2dpa = diphenyl-2,2'-dicarboxylic acid and bpy = 2,2'-bipyridine) was investigated. The nanosized sample of **1** was obtained by sonochemical process. Ultrasound irradiation is well known to accelerate chemical process due to the phenomenon of acoustic cavitation, that is, the formation, growth and collapse of micrometric bubbles, formed by the propagation of a pressure wave through a liquid ultrasound, and its secondary effect, cavitation (nucleation, growth and transient collapse of tiny gas bubbles) improves the mass transfer through convection that is emerged from physical phenomena such as micro-streaming, micro-turbulence, acoustic (or shock) waves and micro jets without significant change in equilibrium characteristics of the adsorption/desorption system. The ultrasound waves create high energy cavitation which can accelerate the reaction duration between solids present in the liquids. Ultrasonic irradiation method required low temperature and less crystallization time compared to hydrothermal heating method [26-29].

MATERIALS AND METHODS

Material

All reagents, including 2,2'-biphenyl dicarboxylic acid (H_2dpa), 2,2'-bipyridine (bpy) and $\text{Cu}(\text{NO}_3)_2\cdot 3\text{H}_2\text{O}$ for the synthesis, were

commercially available and used as received.

Analysis

Equinox 55 FT-IR spectrometer (Bruker, Bremen, Germany) was used to achieve IR spectra in the range of $400\text{-}4000\text{ cm}^{-1}$ with 16 scan's numbers and ATR form. X-ray powder diffraction (XRD) measurements were performed using an X'pert diffractometer manufactured by Philips with monochromatized $\text{Cu K}\alpha$ radiation ($\lambda = 1.54056\text{ \AA}$) with a step size of 0.01671 (degree). The Mercury software was used to prepare simulated XRD powder patterns based on single crystal data. The scanning electron microscope of Philips XL 30 was utilized to characterize the morphology of the samples. The utilized instrument for ultrasonic irradiation was PARSONIC 15S with the frequency of 28 kHz. Melting points were measured on an Electrothermal 9100 apparatus and are uncorrected. Antibacterial activity of samples was determined against Gram-negative bacterial strains *Escherichia coli* (*E. coli*) (ATCC 25922) and Gram-positive bacterial strains *Staphylococcus aureus* (*S. aureus*) (ATCC 25923) using the agar well diffusion assay method. The antibacterial test microorganisms were cultured in nutrient broth for 24 h at $37\text{ }^\circ\text{C}$. Inoculum containing 10^8 CFU/mL of each bacterial culture was incubated on nutrient agar plates by a sterile swab. Subsequently, wells of 4 mm diameter were punched into the agar medium by a sterilized stainless steel cork borer. Compounds were dispersed in 5% DMSO solvent to provide a solution of $50000\text{ }\mu\text{g/mL}$ concentration. Finally, wells were filled with $50\text{ }\mu\text{L}$ of each sample and then plates were incubated at $37\text{ }^\circ\text{C}$ for 24h [30]. The antimicrobial activity of samples was evaluated by comparing the zone of inhibition.

Bulk and sonochemical synthesis of $[\text{Cu}_2(\text{dpa})_2(\text{bpy})_2]\cdot 4\text{H}_2\text{O}$ (**1**)

For the synthesis of a bulk sample of $[\text{Cu}_2(\text{dpa})_2(\text{bpy})_2]\cdot 4\text{H}_2\text{O}$, a solution of 1 mmol (0.242 g) 2,2'-biphenyl dicarboxylic acid (H_2dpa) in 10 mL H_2O and a solution of 2 mmol (0.114 g) potassium hydroxide (KOH) in 5 mL H_2O were prepared. These two solutions were mixed and stirred at $100\text{ }^\circ\text{C}$ for an hour. Then, a prepared solution of 1 mmol (0.156 g) 2,2'-bipyridine (bpy) in 5 mL H_2O was added to the mixture. Obtained solution completely became transparent after a while. Afterward, a prepared solution of 1 mmol (0.242 g) $\text{Cu}(\text{NO}_3)_2\cdot 3\text{H}_2\text{O}$ in 15 mL H_2O was added

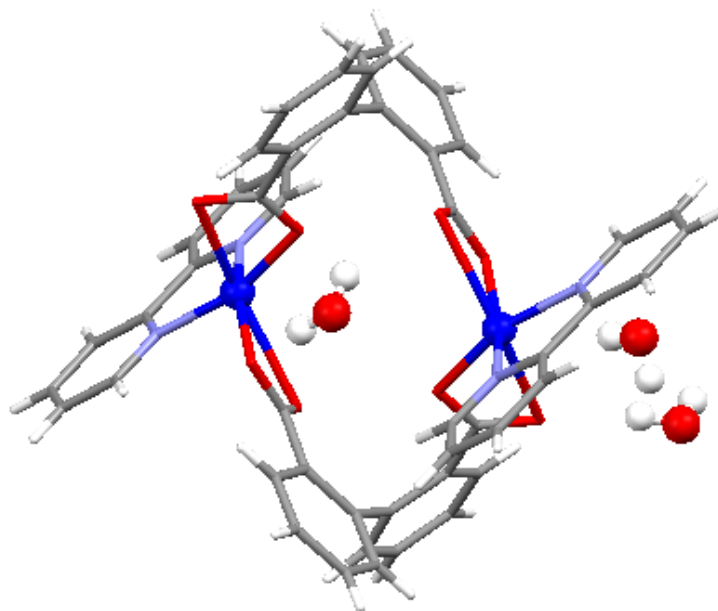


Fig. 1. Molecular structure of metal-organic nanocapsule $[\text{Cu}_2(\text{dpa})_2(\text{bpy})_2]\cdot 4\text{H}_2\text{O}$ (**1**), (Cu: dark blue, N: light blue, C: gray, O: red, H: white).

to the mixture and the mixture was heated and stirred at 100 °C for 1.5 h. The blue precipitates obtained were filtered and washed with water and then dried, d.p. = 240 °C, yield: 0.429 g, 86.5% based on the final product.

To synthesize the sample $[\text{Cu}_2(\text{dpa})_2(\text{bpy})_2]\cdot 4\text{H}_2\text{O}$ sonochemically and obtain nano-structures of the sample, the following procedures were carried out:

A solution of 1 mmol (0.242 g) H_2dpa in 10 mL H_2O and a solution of 2 mmol (0.114 g) potassium hydroxide in 5 mL H_2O were prepared. These two solutions were mixed and stirred at 100 °C for 1 h. Then, a prepared solution of 1 mmol (0.156 g) bpy in 5 mL H_2O was added to the mixture. Obtained solution completely became transparent after a while. Afterward, prepared mixture was put in an ultrasonic bath with the power of 28 kHz and then a solution of 1 mmol (0.242g) $\text{Cu}(\text{NO}_3)_2\cdot 3\text{H}_2\text{O}$ in 15 mL H_2O was added to the mixture in a dropwise manner under the ultrasonic irradiation for 1 h. The blue precipitates obtained were filtered and washed with water and then dried, d.p. = 245 °C, yield: 0.436 g, 87.9% based on the final product [18].

RESULTS AND DISCUSSION

The metal-organic nanocapsule $[\text{Cu}_2(\text{dpa})_2(\text{bpy})_2]\cdot 4\text{H}_2\text{O}$ [23] was synthesized by both the reflux method and the sonochemical process. The structure of the $[\text{Cu}_2(\text{dpa})_2(\text{bpy})_2]\cdot 4\text{H}_2\text{O}$ is a binuclear copper(II) complex that a bpy ligand and two dpa^{2-} ligands are chelated with each copper(II) ion (Fig. 1). Thus, the cluster in the structure of this MONC is a distorted *cis*- $\text{Cu}_2\text{N}_2\text{O}_4$ octahedron [23]. The samples were characterized to investigate the formation of desired products. Then, the antibacterial assessment was carried out on the samples and ligands as controls.

Material characterization
IR spectroscopy

Fig. 2 shows the IR spectra of bulk (Fig. 2a) and the sonochemical prepared sample (Fig. 2b) of $[\text{Cu}_2(\text{dpa})_2(\text{bpy})_2]\cdot 4\text{H}_2\text{O}$ nanocapsule. The conformity of these two spectra approves that both samples have the same structures and have been synthesized successfully. The two strong peaks at 1350 and 1550 cm^{-1} are attributed to the symmetric and asymmetric $-\text{COO}^-$ stretching modes. The peak at 1400 cm^{-1} is attributed to C=C stretching modes of aromatic rings in **1**. The peak at 750 cm^{-1} is attributed to C-H bending mode of aromatic rings in **1**. In addition, the broad band between 2750-3750 cm^{-1} approved the existence of guest H_2O molecules in the pore of compound **1**.

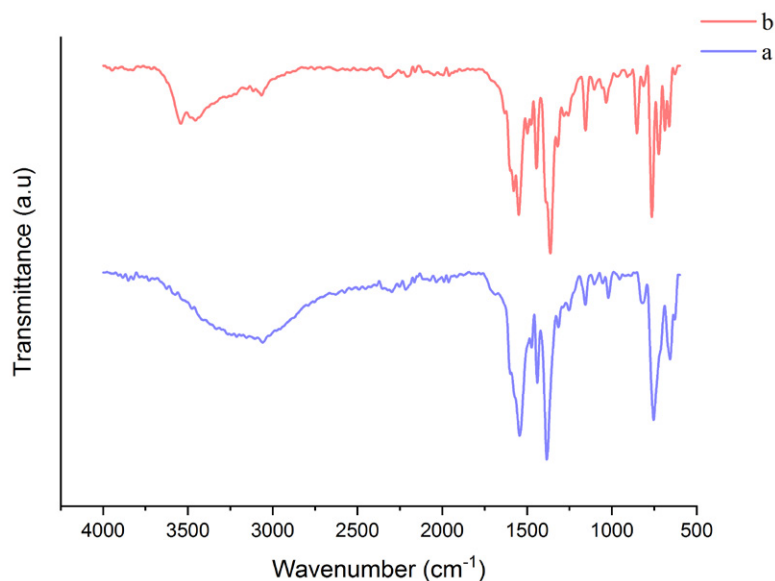


Fig. 2. IR spectra of a) bulk sample of $[\text{Cu}_2(\text{dpa})_2(\text{bpy})_2]\cdot 4\text{H}_2\text{O}$ and b) nanosized sample

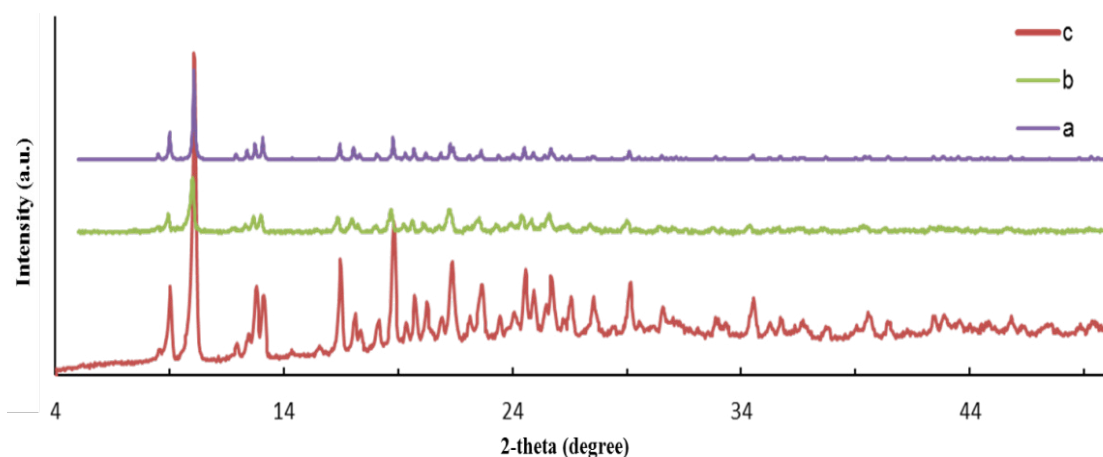


Fig. 3. PXRD patterns. a) Simulated pattern based on single crystal X-ray of $[\text{Cu}_2(\text{dpa})_2(\text{bpy})_2]\cdot 4\text{H}_2\text{O}$ (I), b) bulk sample of I, and c) nanosized sample of I prepared sonochemically.

nanocapsule.

PXRD analysis

The obtained precipitates were characterized by PXRD in order to investigate their crystallinity and purity. As indicated in Fig. 3, the PXRD patterns of the products are in a good agreement with the simulated pattern, indicating that compound **1** has been synthesized successfully by the reflux method and sonochemical process.

SEM

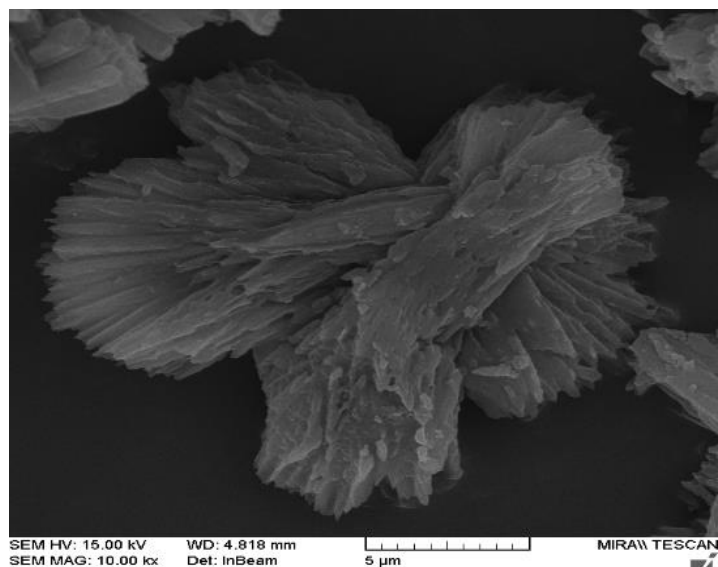
The SEM images of the products display the

morphology and size of the samples obtained by the reflux method and sonochemical process (Fig. 4). Microstructures of **1** were synthesized by the reflux method (Fig. 4a), while nanoparticles of this compound were obtained by the sonochemical process (Fig. 4b).

Antibacterial assay

The antimicrobial potency of the bulk sample of **1** (**1b**) and compound **1** nanoparticles synthesized by sonochemical process (**1s**) was evaluated by agar well diffusion method against *E. coli* and *S. aureus*.

a)



b)

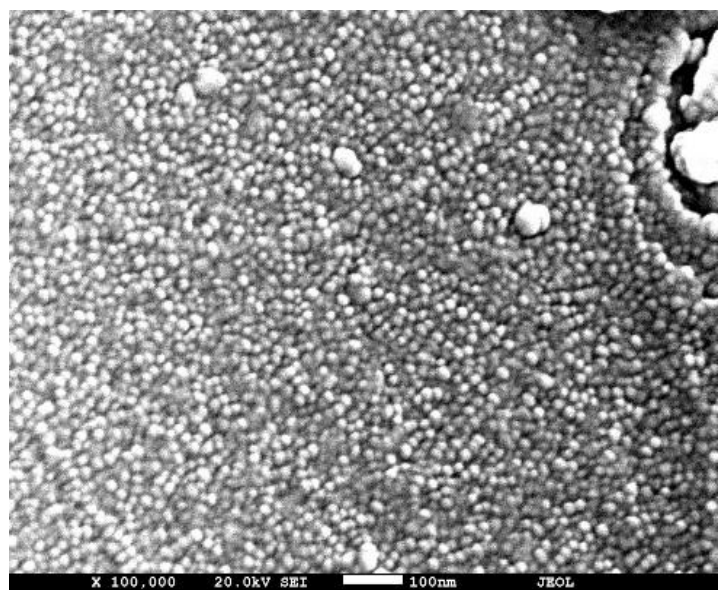


Fig. 4. SEM images of a) bulk sample of **1**, and b) nanosized sample of **1** synthesized by sonochemical process.

The zone of inhibition (ZOI) results of samples, bpy and H₂dpa, are presented in Fig. 5 and Table 1. The results showed that in the case of *E. coli* bacteria, none of the samples and ligands have antibacterial effects except the ligand bpy. The high antibacterial performance of bpy against *E. coli*, and the inert antibacterial performance of samples **1b** and **1s** against *E. coli* bacteria, indicate that ligand release in metal-organic nanocapsule of **1** does not occur.

In the case of *S. aureus*, bpy and both of the bulk and nanosized samples exhibited antimicrobial performance. As indicated in Fig. 5 and also on the basis of measurement of the clear area around samples **1b** and **1s**, the inhibition zone diameter of the nanosized sample is a little bit higher than that of the bulk sample. This fact could be ascribed to the decrease in particle sizes. Decreasing particle size leads to the surface area increase,

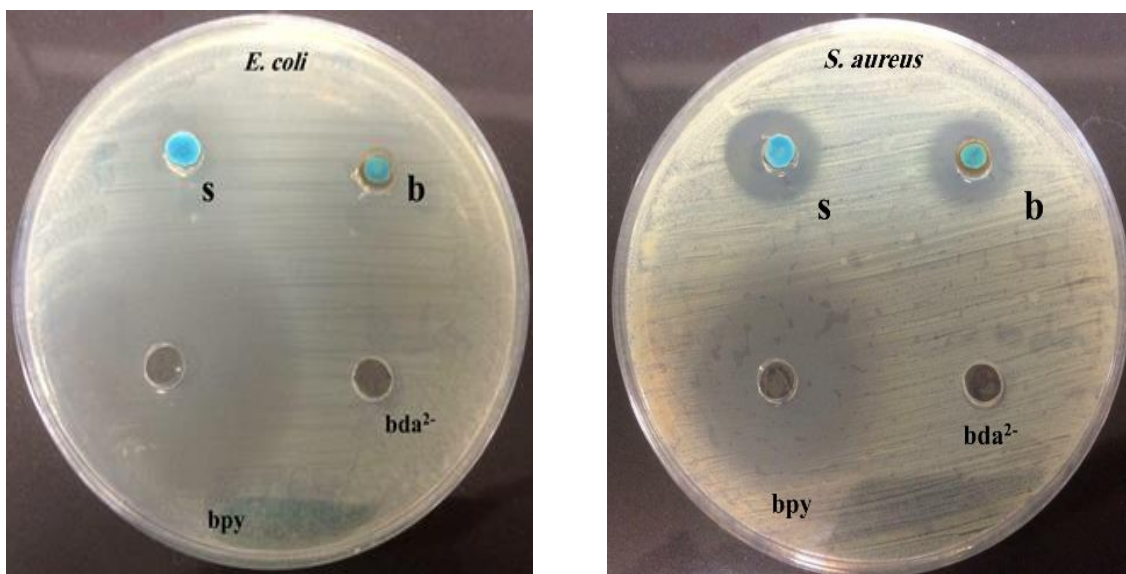


Fig. 5. Antimicrobial activity of the bulk (1b) and nanosized (1s) samples of the metal-organic nanocapsule $[\text{Cu}_2(\text{dpa})_2(\text{bpy})_2]\cdot 4\text{H}_2\text{O}$, bpy, and H_2dpa against *S. aureus* and *E. coli*.

Table 1. Antimicrobial activity of 1b, 1s, bpy, and H_2dpa against *S. aureus* and *E. coli* by agar-well diffusion method.

Samples	Inhibition zone diameter (mm)		Ref.
	<i>S. aureus</i>	<i>E. coli</i>	
1b	13	–	This work
1s	14	–	This work
bpy	20	25	This work
H_2dpa	–	–	This work
$[\text{Ag}_5(\text{PYDC})_2(\text{OH})]$	14	17	[32]
$[\text{Ag}(\text{ace})]_n$	14	-	[33]

resulting in more interaction with the surrounding environment [31]. As indicated in Fig. 5, bpy ligand shows a good antibacterial activity against *S. aureus* bacteria. However, the high chemical stability of **1** resulted in no antibacterial activity of **1** against *E. coli* bacteria. Thus, it could be concluded that the antibacterial property of **1** is not attributed to Cu^{2+} or the bpy release from **1**. The antibacterial activity of **1** against *S. aureus* might be due to surface Cu^{2+} metal ions with broken coordination bonds and the existence of open metal sites in the surface of the particles that resulted in more interaction with *S. aureus* bacteria.

The results also indicate that antibacterial activities of 1b and 1s are comparable to the other reported compounds. The reported inhibition zone of area for $[\text{Ag}_5(\text{PYDC})_2(\text{OH})]$ [32] and $[\text{Ag}(\text{ace})]_n$ [33] against *S. aureus* is 14 mm that is equal to the

inhibition zone of 1s for *S. aureus*.

CONCLUSION

Metal-organic nanocapsules (MONCs) are as active as other organic-inorganic compounds against pathogens. Thus, $[\text{Cu}_2(\text{dpa})_2(\text{bpy})_2]\cdot 4\text{H}_2\text{O}$ (**1**) MONC was chosen to investigate the antimicrobial activity of its bulk and nanosized samples against *S. aureus* and *E. coli*. Also, this compound was chosen among other MONCs due to its metal ion and the solvent (water) used for its synthesis. The bulk and nanosized samples of $[\text{Cu}_2(\text{dpa})_2(\text{bpy})_2]\cdot 4\text{H}_2\text{O}$ (**1**) were prepared and their antimicrobial performances were evaluated by agar well diffusion method. The results of the antimicrobial assay showed that both bulk and nanosized samples are active against *S. aureus* bacteria. However, they were inert against *E. coli*. The inhibition zone diameter of the nanosized

sample is a little bit higher than the bulk sample. The bpy ligand is active against both strains of bacteria. It seems that no bpy and subsequently no Cu(II) release has occurred as a result of high chemical stability of **1**. Furthermore, the good antibacterial activity of **1** against *S. aureus* bacteria could be attributed to the surface Cu²⁺ metal ions with broken coordination bonds and the existence of Cu²⁺ metal ions with an open metal site on the surface of compound **1** particles, that resulted in more interactions with *S. aureus* bacteria.

ACKNOWLEDGEMENTS

The authors would like to acknowledge the financial support of University of Tehran for this research under grant number 01/1/389845.

CONFLICT OF INTEREST

The authors confirm that this article content has no conflict of interest.

REFERENCES

- Holt BA, Gregory SA, Sulchek T, Yee S, Losego MD. Aqueous Zinc Compounds as Residual Antimicrobial Agents for Textiles. *ACS Applied Materials & Interfaces*. 2018;10(9):7709-16.
- Harding JL, Reynolds MM. Combating medical device fouling. *Trends in Biotechnology*. 2014;32(3):140-6.
- Kenawy E-R, Worley SD, Broughton R. The Chemistry and Applications of Antimicrobial Polymers: A State-of-the-Art Review. *Biomacromolecules*. 2007;8(5):1359-84.
- Mousavi Khaneghah A, Hashemi SMB, Limbo S. Antimicrobial agents and packaging systems in antimicrobial active food packaging: An overview of approaches and interactions. *Food and Bioproducts Processing*. 2018;111:1-19.
- Sung S-Y, Sin LT, Tee T-T, Bee S-T, Rahmat AR, Rahman WAWA, et al. Antimicrobial agents for food packaging applications. *Trends in Food Science & Technology*. 2013;33(2):110-23.
- Wyszogrodzka G, Marszałek B, Gil B, Dorożyński P. Metal-organic frameworks: mechanisms of antibacterial action and potential applications. *Drug Discovery Today*. 2016;21(6):1009-18.
- Jo JH, Kim H-C, Huh S, Kim Y, Lee DN. Antibacterial activities of Cu-MOFs containing glutarates and bipyridyl ligands. *Dalton Transactions*. 2019;48(23):8084-93.
- Cattaneo C, Di Blasi R, Skert C, Candoni A, Martino B, Di Renzo N, et al. Bloodstream infections in haematological cancer patients colonized by multidrug-resistant bacteria. *Annals of Hematology*. 2018;97(9):1717-26.
- Ximing G, Bin G, Yuanlin W, Shuanghong G. Preparation of spherical metal-organic frameworks encapsulating ag nanoparticles and study on its antibacterial activity. *Materials Science and Engineering: C*. 2017;80:698-707.
- Chowdhuri AR, Das B, Kumar A, Tripathy S, Roy S, Sahu SK. One-pot synthesis of multifunctional nanoscale metal-organic frameworks as an effective antibacterial agent against multidrug-resistant *Staphylococcus aureus*. *Nanotechnology*. 2017;28(9):095102.
- Miranzadeh M, Kassae M, Afshari F. Efficiency of Cu, Ag, and Fe Nanoparticles As Detergents Preservatives Against *E. coli* and *S. aureus*. *Nanochemistry Research*. 2020;4(2):170-8.
- Sorbiun M, Shayegan Mehr E, Ramazani A, Mashhadi Malekzadeh A. Biosynthesis of metallic nanoparticles using plant extracts and evaluation of their antibacterial properties. *Nanochemistry Research*. 2018;3(1):1-16.
- Ren X, Yang C, Zhang L, Li S, Shi S, Wang R, et al. Copper metal-organic frameworks loaded on chitosan film for the efficient inhibition of bacteria and local infection therapy. *Nanoscale*. 2019;11(24):11830-8.
- Dizaj SM, Lotfipour F, Barzegar-Jalali M, Zarrintan MH, Adibkia K. Antimicrobial activity of the metals and metal oxide nanoparticles. *Materials Science and Engineering: C*. 2014;44:278-84.
- Ahamed M, Alhadlaq HA, Khan MAM, Karuppiah P, Al-Dhabi NA. Synthesis, Characterization, and Antimicrobial Activity of Copper Oxide Nanoparticles. *Journal of Nanomaterials*. 2014;2014:1-4.
- Restrepo J, Serroukh Z, Santiago-Morales J, Aguado S, Gómez-Sal P, Mosquera MEG, et al. An Antibacterial Zn-MOF with Hydrazinebenzoate Linkers. *European Journal of Inorganic Chemistry*. 2016;2017(3):574-80.
- Zhao Y, Jiang L. Hollow Micro/Nanomaterials with Multilevel Interior Structures. *Advanced Materials*. 2009;21(36):3621-38.
- Mirzadeh E, Akhbari K. Reversible adsorption and desorption of water in nanoporous copper(II) metal-organic nanocapsules. *Journal of Porous Materials*. 2017;24(5):1209-14.
- Yun G, Hassan Z, Lee J, Kim J, Lee N-S, Kim NH, et al. Highly Stable, Water-Dispersible Metal-Nanoparticle-Decorated Polymer Nanocapsules and Their Catalytic Applications. *Angewandte Chemie International Edition*. 2014;53(25):6414-8.
- Wang X-W, Gao W, Fan H, Ding D, Lai X-F, Zou Y-X, et al. Simultaneous tracking of drug molecules and carriers using aptamer-functionalized fluorescent superstable gold nanorod-carbon nanocapsules during thermo-chemotherapy. *Nanoscale*. 2016;8(15):7942-8.
- Jang J, Oh JH. Facile Fabrication of Photochromic Dye-Conducting Polymer Core-Shell Nanomaterials and Their Photoluminescence. *Advanced Materials*. 2003;15(12):977-80.
- Nouri R, Tahmasebi E, Morsali A. Capability of magnetic functional metal-organic nanocapsules for removal of mercury(II) ions. *Materials Chemistry and Physics*. 2017;198:310-6.
- Tang L, Shi J, Wang X, Zhang S, Wu H, Sun H, et al. Coordination polymer nanocapsules prepared using metal-organic framework templates for pH-responsive drug delivery. *Nanotechnology*. 2017;28(27):275601.
- Zhang C, Sikligar K, Patil RS, Barnes CL, Baker GA, Atwood JL. A M18L6 metal-organic nanocapsule with open windows using mixed macrocycles. *Chemical Communications*. 2018;54(6):635-7.
- He H-Y, Zhou Y-L, Gao J. Bis(μ -biphenyl-2,2'-dicarboxylato) bis[(2,2'-bipyridine)copper(II)] tetrahydrate. *Acta Crystallographica Section E Structure Reports Online*. 2007;63(7):m2007-m.

26. Yeroslavsky G, Richman M, Dawidowicz L-o, Rahimpour S. Sonochemically produced polydopamine nanocapsules with selective antimicrobial activity. *Chemical Communications*. 2013;49(51):5721.
27. Shahangi Shirazi F, Akhbari K, Kawata S, Ishikawa R. Effects of different factors on the formation of nanorods and nanosheets of silver(I) coordination polymer. *Journal of Molecular Structure*. 2016;1123:206-12.
28. Amara N, Ratsimba B, Wilhelm A-M, Delmas H. Crystallization of potash alum: effect of power ultrasound. *Ultrasonics Sonochemistry*. 2001;8(3):265-70.
29. Enomoto N, Maruyama S, Nakagawa Z-e. Agglomeration of silica spheres under ultrasonication. *Journal of Materials Research*. 1997;12(5):1410-5.
30. Restrepo J, Serroukh Z, Santiago-Morales J, Aguado S, Gómez-Sal P, Mosquera MEG, et al. An Antibacterial Zn-MOF with Hydrazinebenzoate Linkers. *European Journal of Inorganic Chemistry*. 2016;2017(3):574-80.
31. Sau TK, Rogach AL, Jäckel F, Klar TA, Feldmann J. Properties and Applications of Colloidal Nonspherical Noble Metal Nanoparticles. *Advanced Materials*. 2010;22(16):1805-25.
32. Lu X, Ye J, Zhang D, Xie R, Bogale RF, Sun Y, et al. Silver carboxylate metal-organic frameworks with highly antibacterial activity and biocompatibility. *Journal of Inorganic Biochemistry*. 2014;138:114-21.
33. Cavicchioli M, Massabni AC, Heinrich TA, Costa-Neto CM, Abrão EP, Fonseca BAL, et al. Pt(II) and Ag(I) complexes with acesulfame: Crystal structure and a study of their antitumoral, antimicrobial and antiviral activities. *Journal of Inorganic Biochemistry*. 2010;104(5):533-40.